Electronic Supplementary Information (ESI)

A new meso-porous coordination polymer: synthesis, structure, and gas adsorption studies

Jingui Duan,*[a] Qianqian Li,[a] Zhiyong Lu,[b]

[a] *State Key Laboratory of Materials-Oriented Chemical Engineering, College of Chemistry and Chemical engineering, Nanjing Tech University, Nanjing, 210009, China. E-mail: duanjingui@njtech.edu.cn*

[b] *State Key Laboratory of Coordination Chemistry, School of Chemistry and Chemical Engineering, Nanjing University, Nanjing 210093, PR China*

General Information. All the reagents and solvents were commercially available and used as received. The IR spectra were recorded in the range of 4000-400 cm^{-1} on a Nicolet ID5 ATR spectrometer. The elemental analysis was carried out with a Perkin-Elmer 240C elemental analyzer. Thermal analyses were performed on a Rigaku TG8120 instrument from room temperature to 600 °C at a heating rate of 5 °C/min under flowing nitrogen. Powder X-ray diffraction was obtained using a Rigaku RINT powder diffractometer with Cu Kα anode. The simulated PXRD spectra were acquired by the diffraction-crystal module of the Mercury program based on the single-crystal data. The program is available free of charge via the Internet at http://www.iucr.org.

Synthesis of the organic building block. 1,3,5-Tri(6-hydroxycarbonylnaphthalen -2-yl)benzene (H_3BTN) was synthesized according to the our previous work[1].

Synthesis of NJTU-1. H_3BTN (6 mg, 0.01 mmol), $Cu(NO_3)_2 \cdot 3H_2O$ (15 mg, 0.062 mmol), DMF/H_2O = 5:1 (1 mL), and concentrated HNO_3 (30 μL) were mixed and stirred for a few minutes in air and then the clear solution was transferred into a autoclave Teflon-line stainless vessel (4 mL). The vessel was sealed and heated at 65

°C for 2 days and then cooled to room temperature. Green block crystals of NJTU-1 were obtained and then washed by DMF (yield: ~60% based on ligand). Anal. Calcd. $C_{26}H_{14}CuO4$: C, 68.79; H, 3.11%.Found: C, 67.21; H, 2.95%.

Single Crystal X-ray Study. Single-crystal X-ray diffraction data were measured on a Bruker Smart Apex CCD diffractometer at 223 K using graphite monochromated Mo/Kα radiation (λ = 0.71073 Å). Data reduction was made with the Bruker Saint program. The structure was solved by direct methods and refined using the full-matrix least squares technique using the SHELXTL package[2]. Nonhydrogen atoms were refined with anisotropic displacement parameters during the final cycles. Organic hydrogen atoms were placed in calculated positions with isotropic displacement parameters set to 1.2Ueq of the attached atom. The unit cell includes a large region of disordered solvent molecules, which could not be modeled as discrete atomic sites. We employed PLATON/SQUEEZE[3] to calculate the diffraction contribution of the solvent molecules and, thereby, to produce a set of solvent-free diffraction intensities; the structure was then refined again using the data generated.

Sample Activation. Before the supercritical CO_2 treatment, as-synthesized samples were soaked in absolute DMF, replacing the soaking solution every 24 h for 3 days. After exchanging, the DMF-containing samples were placed inside the supercritical CO_2 dryer and the DMF was exchanged with CO_2 over a period of 4 h. During this time the liquid CO_2 was vented under positive pressure for five minutes every two hours. The rate of venting of CO_2 was always kept below the rate of filling so as to maintain a full drying chamber. Following venting, the chamber was sealed and the temperature was raised to 40 ºC, at which time the chamber was slowly vented over the course of 15 h. The color of the NJTU-1 changed from green to blue. The collected sample was transferred into the sample tube and activated under a dynamic high vacuum at room temperature for a overnight to obtain the desolvated sample.

Adsorption Experiments. In the low pressure gas sorption measurement, ultra-high-purity grade were used throughout the adsorption experiments. Gas adsorption isotherms were obtained using a Belsorp-mini volumetric adsorption instrument from BEL Japan Inc. using the volumetric technique. A part of the N_2 sorption isotherm at

77 K in the P/P_0 range 0.02-0.08 was fitted to the BET equation to estimate the BET surface area, and the Langmuir surface area calculation was performed using all data points. The pore-size distribution was obtained from the DFT model (assuming split pore geometry) based on the N_2 sorption isotherm. High pressure adsorption of CO_2, CH_4, C_2H_4 and C_2H_6 were measured by using a Belsorp-HP adsorption instrument at 273 and 298 K, respectively. The total high-pressure gas uptake was calculated by $N_{total} = N_{excess} + \rho_{bulk} V_{pore}$, where ρ_{bulk} is the density of compressed gas at the measured temperature and V_{pore} (1.0635 $cm^3 \cdot g^{-1}$) is the pore volume of the sample that was obtained from the N_2 isotherm at 77 K.

Selectivity prediction for binary mixture adsorption. Ideal adsorbed solution theory (IAST) [4] was used to predict binary mixture adsorption from the experimental pure-gas isotherms. In order to perform the integrations required by IAST, the single-component isotherms should be fitted by a proper model. There is no restriction on the choice of the model to fit the adsorption isotherm, but data over the pressure range under study should be fitted very precisely [5]. Several isotherm models were tested to fit the experimental pure isotherms for CH_4, C_2H_4, C_2H_6 and CO_2 of NJTU-1, and the dual-site Langmuir-Freundlich equation were found to best fit the experimental data:

$$q = q_{m1} \cdot \frac{b_1 \cdot P^{1/n_1}}{1 + b_1 \cdot P^{1/n_1}} + q_{m2} \cdot \frac{b_2 \cdot P^{1/n_2}}{1 + b_2 \cdot P^{1/n_2}} \quad (1)$$

Here, P is the pressure of the bulk gas at equilibrium with the adsorbed phase (kPa), q is the adsorbed amount per mass of adsorbent (mol/kg), q_{m1} and q_{m2} are the saturation capacities of sites 1 and 2 (mol/kg), b_1 and b_2 are the affinity coefficients of sites NJTU-1 (1/kPa), and n_1 and n_2 represent the deviations from an ideal homogeneous surface. Figure. 4 shows that the dual-site Langmuir-Freundlich equation fits the single-component isotherms extremely well. The R^2 values for all the fitted isotherms were over 0.9998. Hence, the fitted isotherm parameters were applied to perform the necessary integrations in IAST.

Estimation of the isosteric heats of gas adsorption. A virial-type expression comprising the temperature-independent parameters a_i and b_i was employed to

calculate the enthalpies of adsorption for CO_2 (at 273 and 298 K) on NJTU-1. The data were fitted using the equation:

$$\ln P = \ln N + 1/T \sum_{i=0}^{m} a_i N^i + \sum_{i=0}^{n} b_i N^i \quad (1)$$

Here, P is the pressure expressed in Torr, N is the amount adsorbed in mmol/g, T is the temperature in K, a_i and b_i are virial coefficients, and m, n represent the number of coefficients required to adequately describe the isotherms (m and n were gradually increased until the contribution of extra added a and b coefficients was deemed to be statistically insignificant towards the overall fit, and the average value of the squared deviations from the experimental values was minimized).

$$Q_{st} = -R \sum_{i=0}^{m} a_i N^i \quad (2)$$

Here, Q_{st} is the coverage-dependent isosteric heat of adsorption and R is the universal gas constant. In addition, the determination of the Q_{st} on MgMOF-74, NiMOF-74, Cu-TDPAT, CuBTC, and NaX zeolite is based on other reported paper[6].

Calculations of adsorption selectivity. The selectivity of preferential adsorption of component 1 over component 2 in a mixture containing 1 and 2, perhaps in the presence of other components too, can be formally defined as

$$S_{ads} = \frac{q_1/q_2}{p_1/p_2} \quad (3)$$

In equation (3), q_1 and q_2 are the *absolute* component loadings of the adsorbed phase in the mixture. In all the calculations to be presented below, the calculations of S_{ads} are based on the use of the Ideal Adsorbed Solution Theory of Myers and Prausnitz[7].

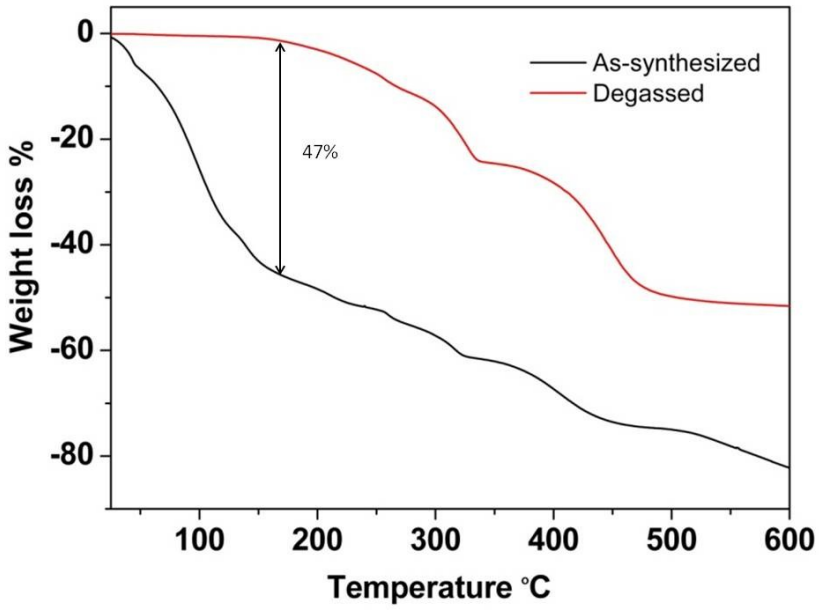

Figure S1. TG of NJTU-1**:** as-synthesized samples (black) and completely activated samples (red).

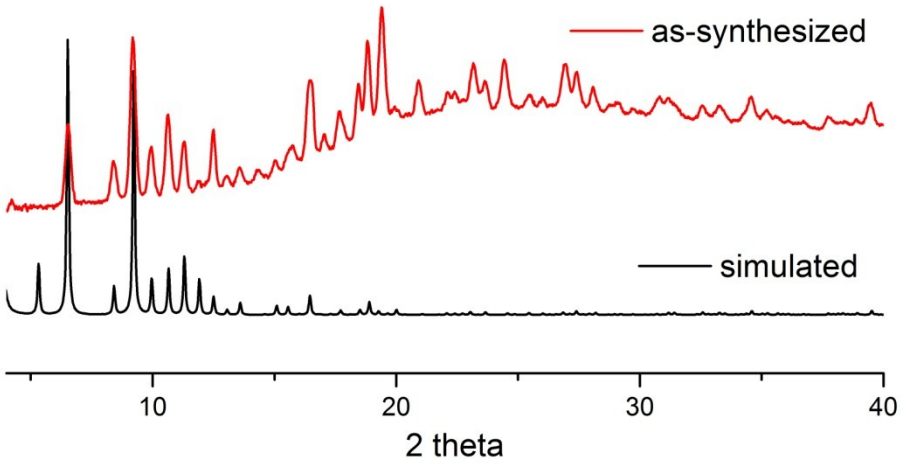

Figure S2. The PXRD patterns of NJTU-1.

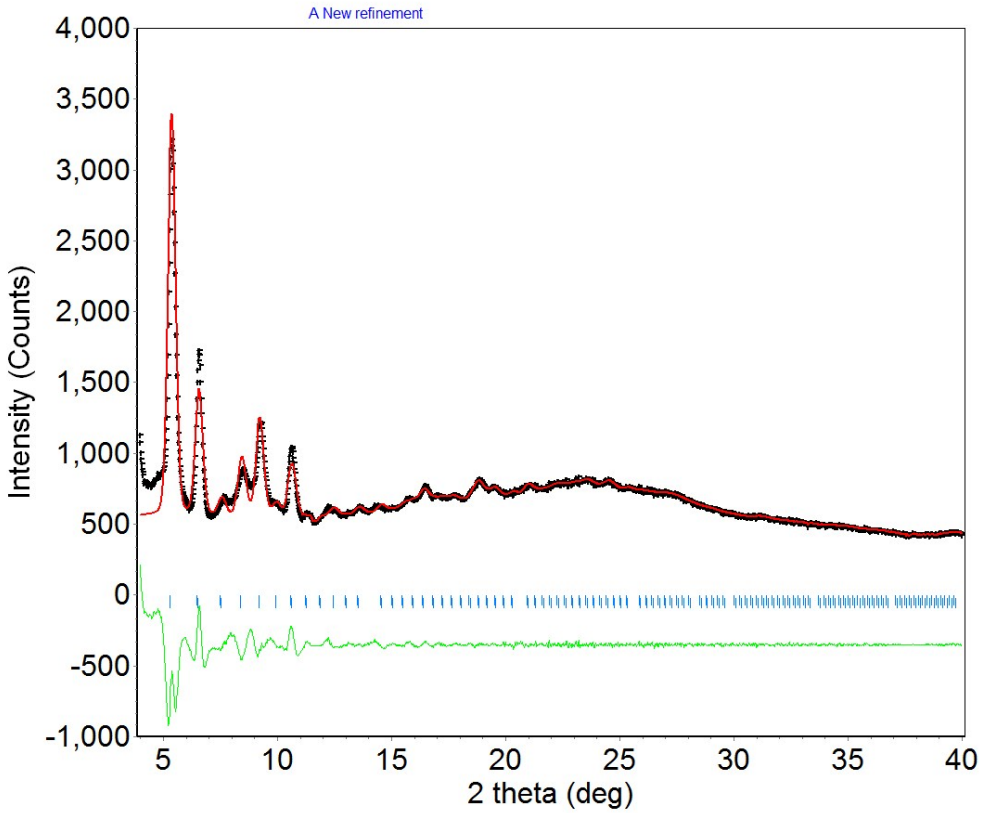

Figure S3. The results of Le Bail analysis for the PXRD of activated NJTU-1 by S-CO_2. Refined parameters and reliability factors are as follows: space group: Im-3, a = 33.3895 Å; R_p = 0.03892 and R_{wp} = 0.08044.

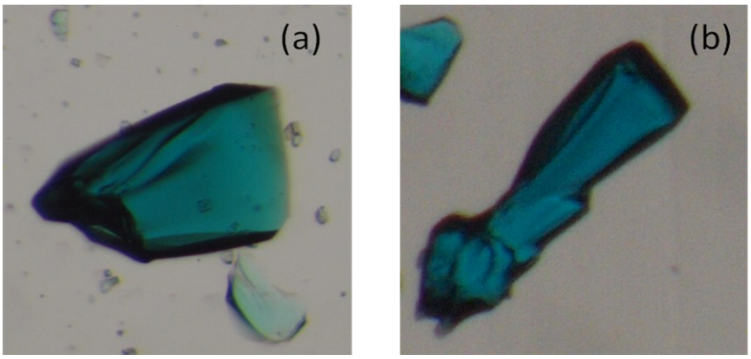

Figure S4. Photographic images of NJTU-1. (a): as-synthesized; (b) Activated samples by S-CO_2.

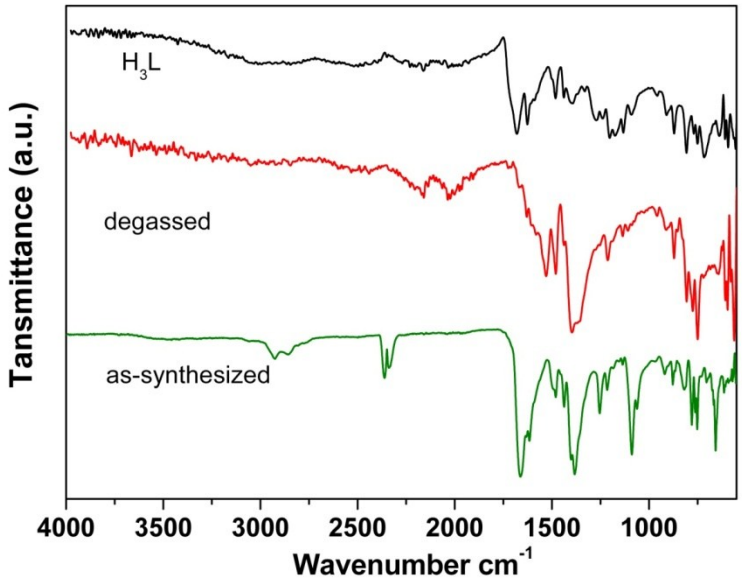

Figure S5. Infrared spectra of the ligand, as-synthesized and degassed form of NJTU-1.

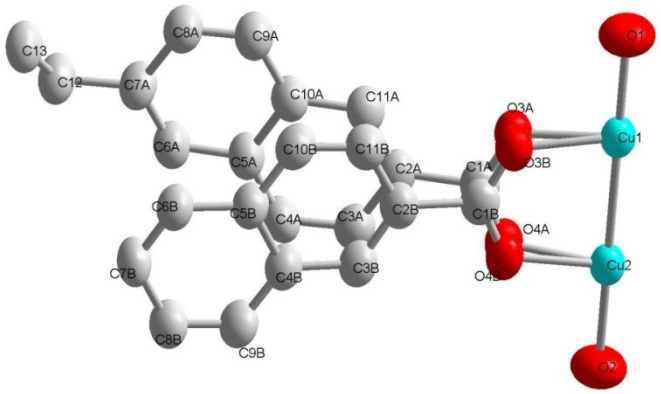

Figure S6. ORTEP View of the asymmetric unit for NJTU-1**.**

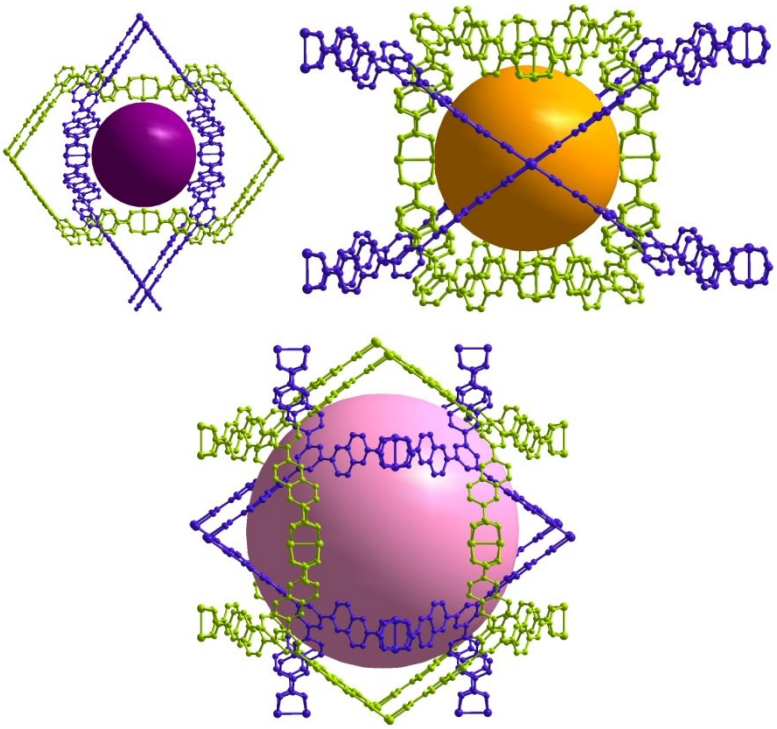

Figure S7. Three types of interpenetrated cage in NJTU-1.

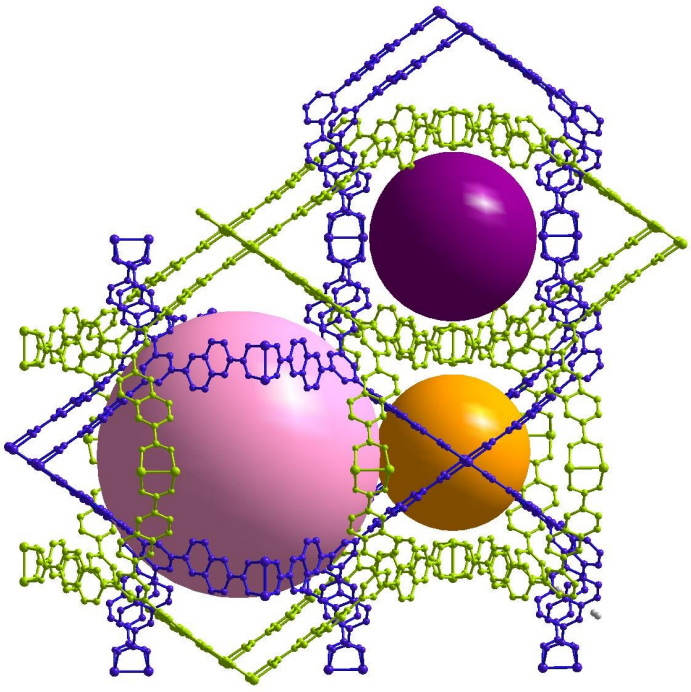

Figure S8. The packing of three types of interpenetrated cage in NJTU-1.

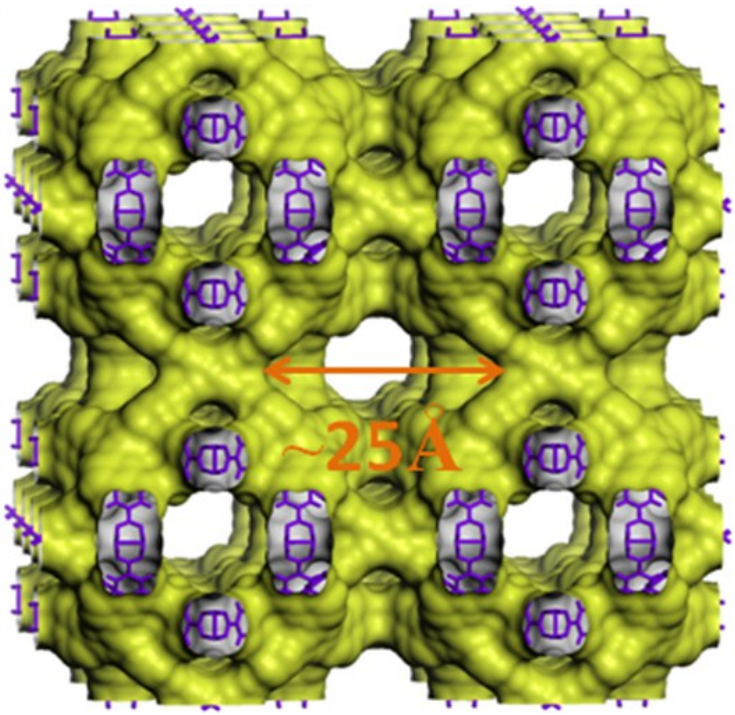

Figure S9. The Connolly surface diagram displays the large three dimensional cross-linking tunnels in NJTU-1 (inner surfaces: yellow, outer surfaces: grey).

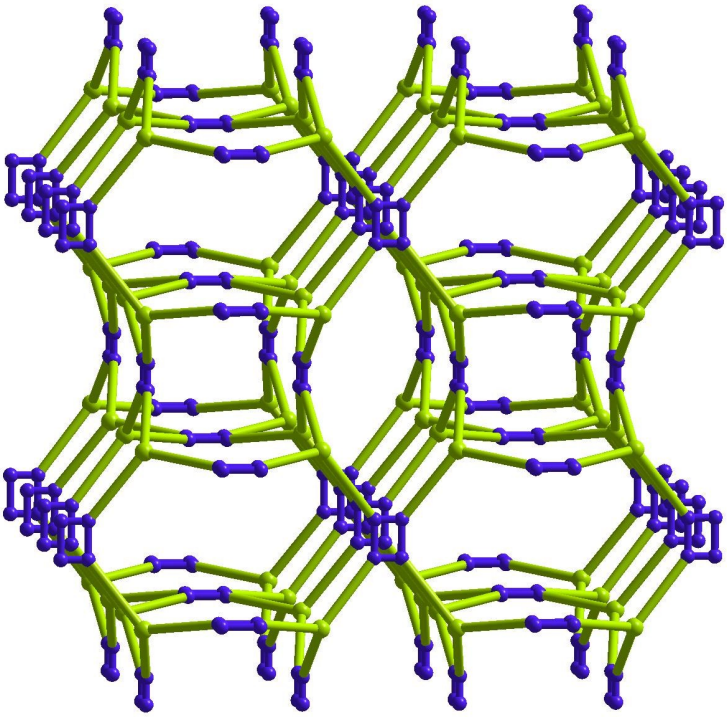

Figure S10. The *sqc* topology of NJTU-1.

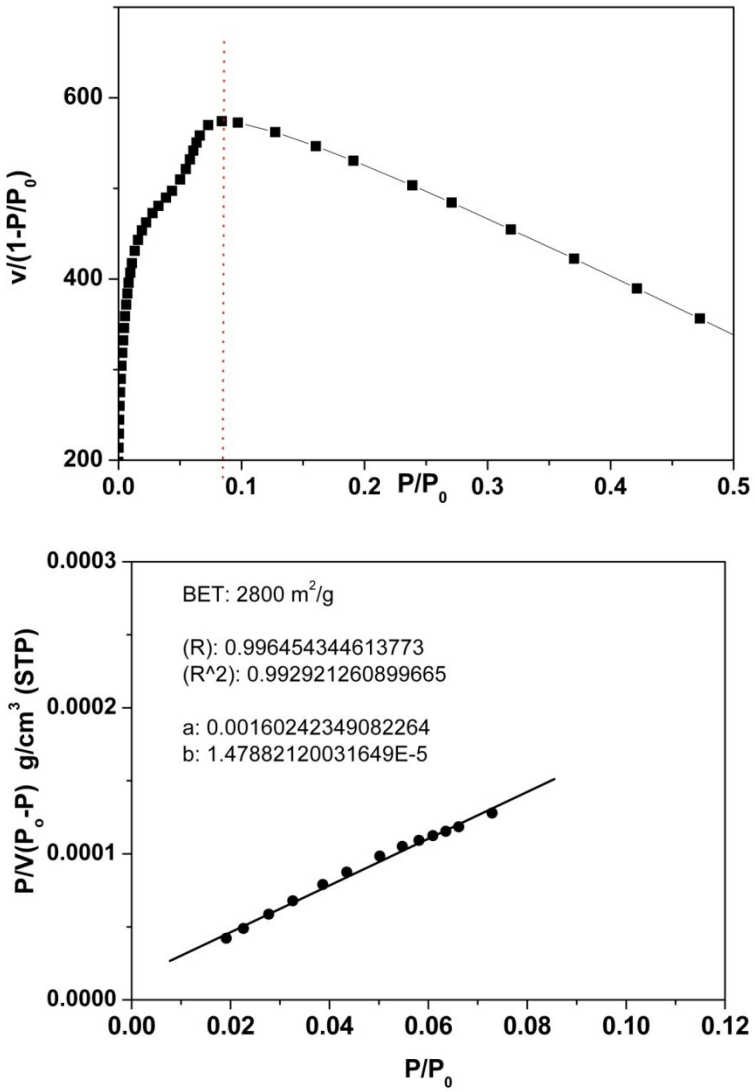

Figure S11. The upper figure shows the consistency plot to determine the pressure range for BET fitting, and the bottom is the calculated BET plot from N_2 isotherm of NJTU-1.

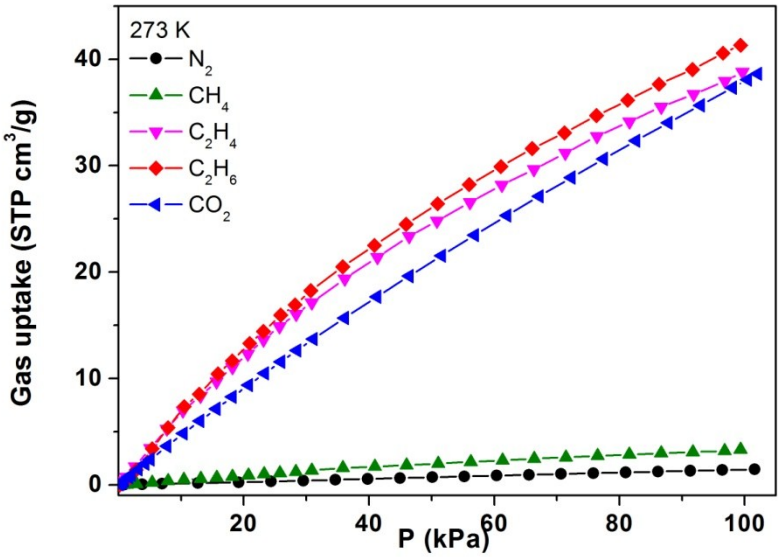

Figure S12. Series gases adsorption isotherm of NJTU-1 at 273, respectively.

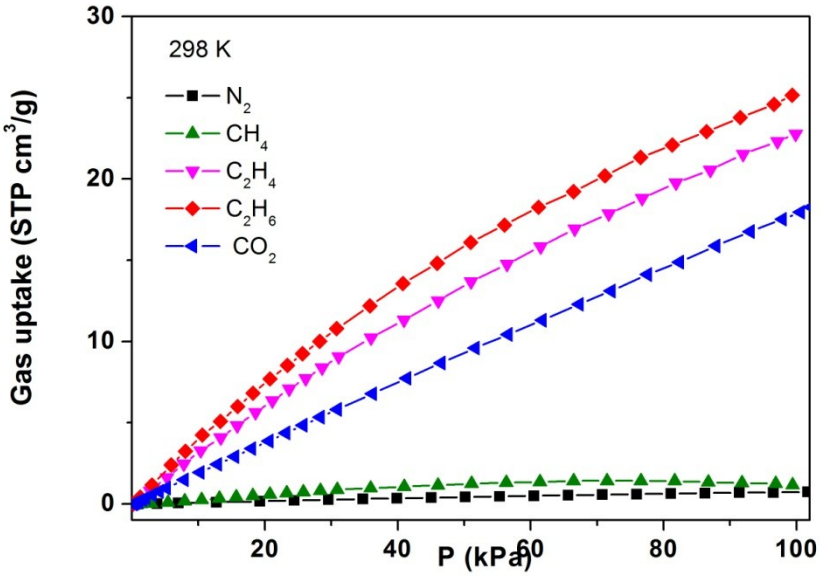

Figure S13. Series gases adsorption isotherm of NJTU-1 at 298, respectively.

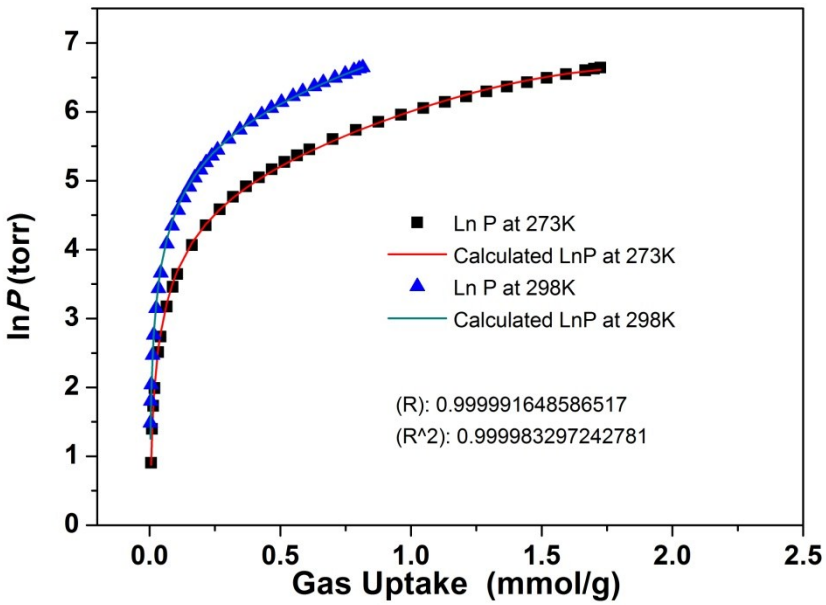

Figure S14. The calculated virial equation isotherms parameters fit to the experimental CO_2 data of NJTU-1.

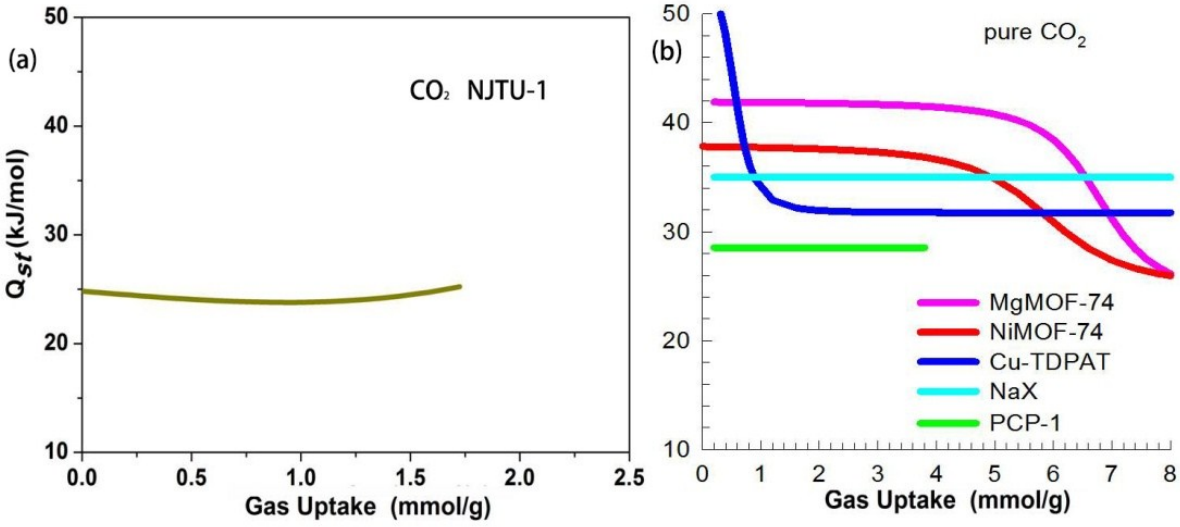

Figure S15. The isosteric heat of adsorption for CO_2 in series PCPs.

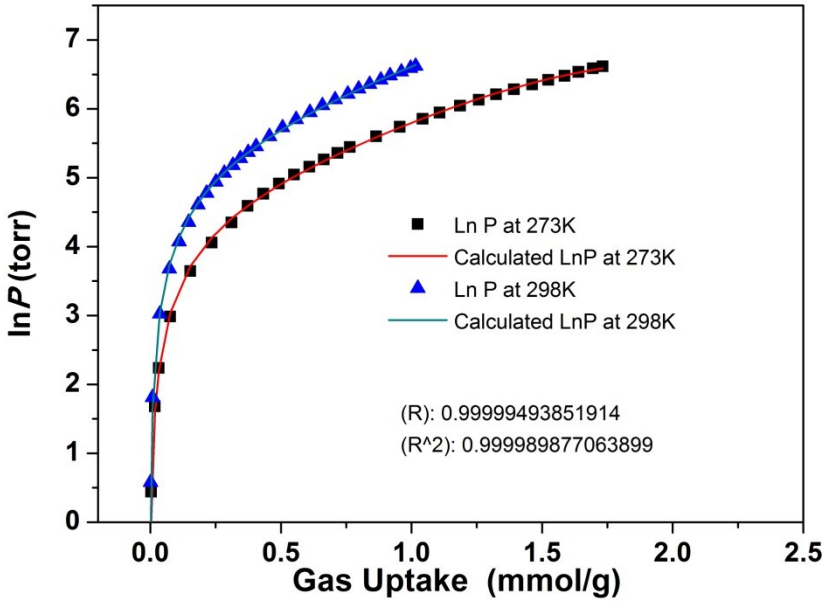

Figure S16. The calculated virial equation isotherms parameters fit to the experimental C_2H_4 data of NJTU-1.

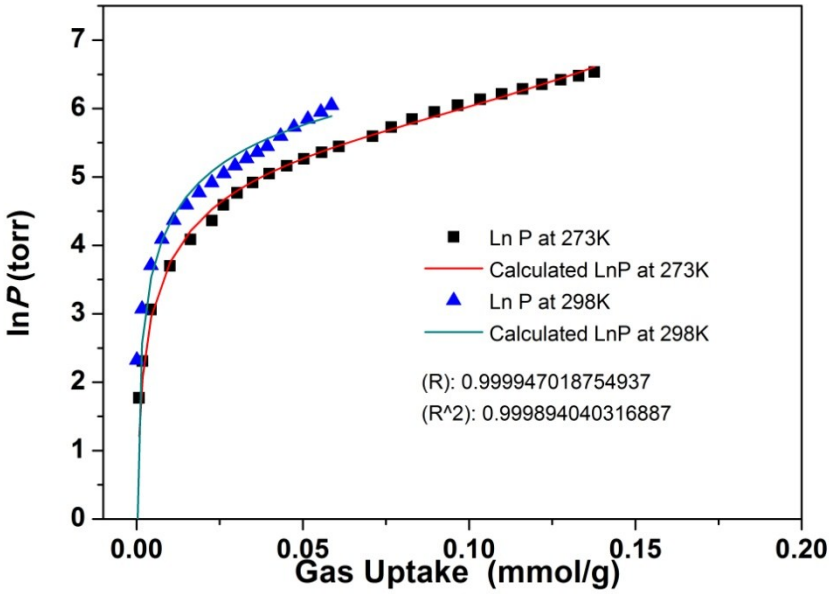

Figure S17. The calculated virial equation isotherms parameters fit to the experimental CH_4 data of NJTU-1.

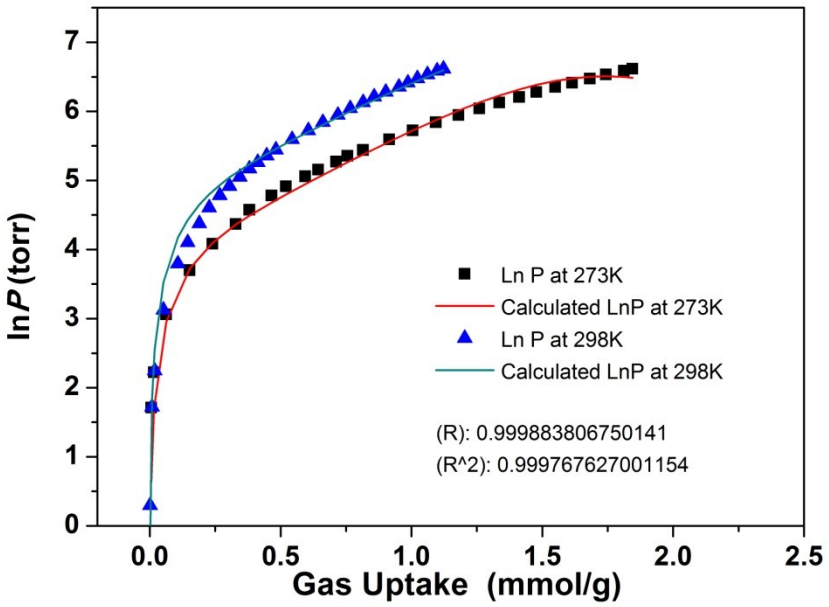

Figure S18. The calculated virial equation isotherms parameters fit to the experimental C_2H_6 data of NJTU-1.

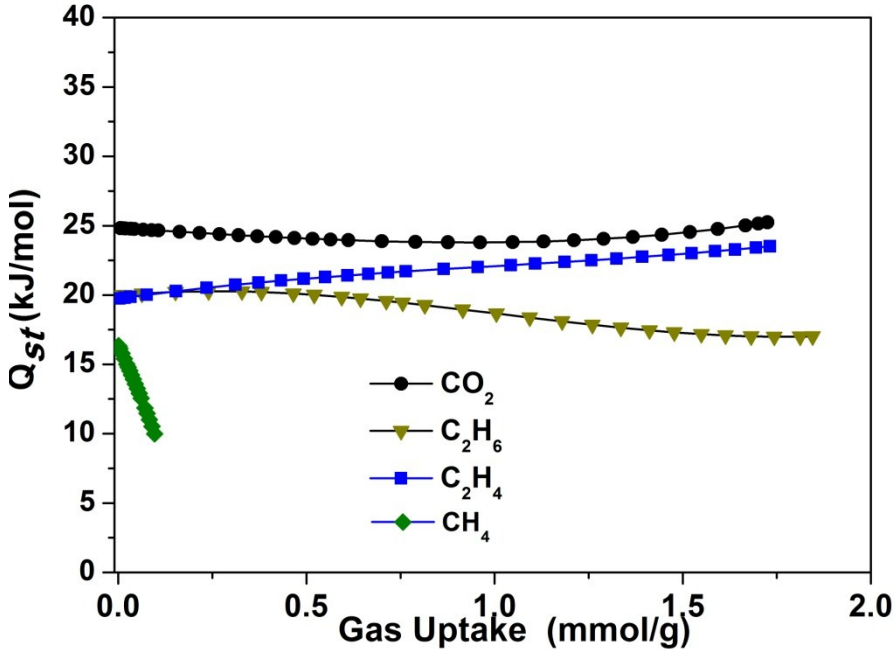

Figure S19. The isosteric heat of series gases in NJTU-1.

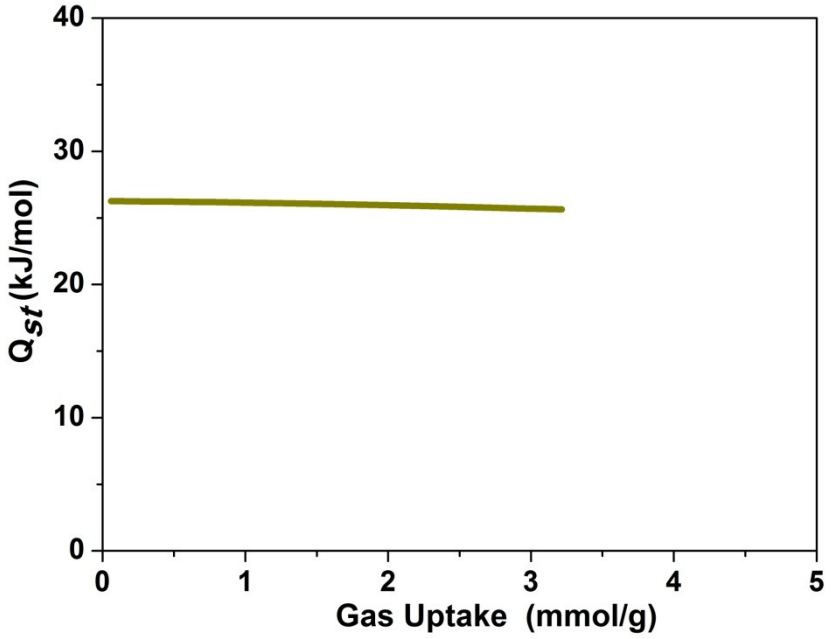

Figure S20. The isosteric heat of CO_2 in MOF-14.

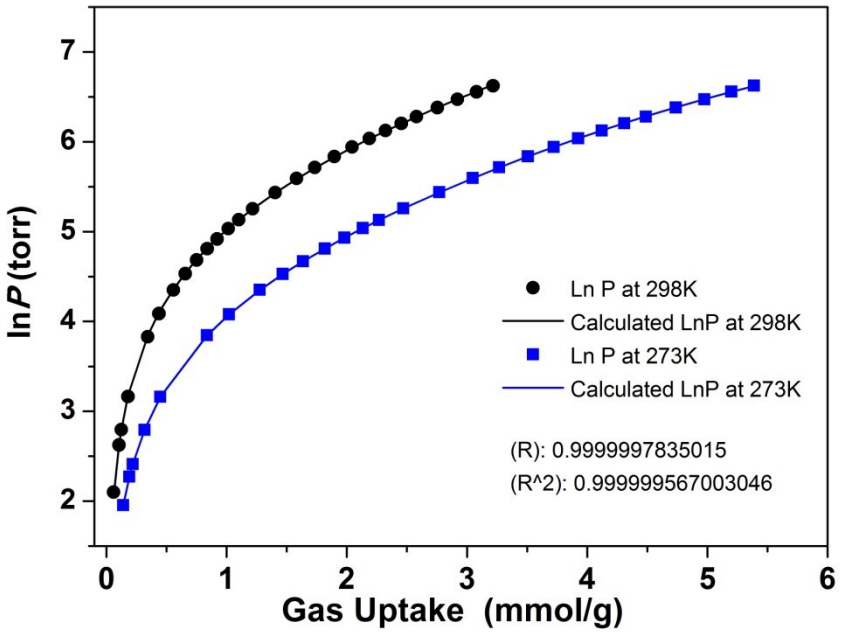

Figure S21. The calculated virial equation isotherms parameters fit to the experimental CO_2 data of MOF-14.

Reference

1. J. G. Duan, M. Higuchi, R. Krishna, T. Kiyonaga, Y. Tsutsumi, Y. Sato, Y. Kubota, M. Takata and S. Kitagawa, *Chem Sci*, 2014, **5**, 660-666.
2. G. M. Sheldrick, *Acta Crystallogr. Sec. A* 2008, **64**, 112-122.
3. A. L. Spek, *PLATON, A Multipurpose Crystallographic Tool (Utrecht University,2001).*
4. (a)Y. S. Bae, K. L. Mulfort, H. Frost, P. Ryan, S. Punnathanam, L. J. Broadbelt, J. T. Hupp and R. Q. Snurr, *Langmuir*, 2008, **24**, 8592-8598; (b)N. F. Cessford, N. A. Seaton and T. Duren, *Ind. Eng. Chem. Res.*, 2012, **51**, 4911-4921.
5. (a)R. Babarao, Z. Q. Hu, J. W. Jiang, S. Chempath and S. I. Sandler, *Langmuir*, 2007, **23**, 659-666; (b)V. Goetz, O. Pupier and A. Guillot, *Adsorption*, 2006, **12**, 55-63.
6. (a)H. Wu, K. Yao, Y. Zhu, B. Li, Z. Shi, R. Krishna and J. Li, *J. Phys. Chem. C*, 2012, **116**, 16609-16618; (b)S. C. Xiang, Y. He, Z. Zhang, H. Wu, W. Zhou, R. Krishna and B. Chen, *Nat. Commun.*, 2012, **3**, 954; (c)Y. He, R. Krishna and B. Chen, *Energy Environ. Sci.*, 2012, **5**, 9107-9120; (d)Y. He, S. Xiang, Z. Zhang, S. Xiong, C. Wu, W. Zhou, T. Yildirim, R. Krishna and B. Chen, *J. Mater. Chem. A*, 2013, **1**, 2543-2551.
7. A. L. Myers and J. M. Prausnitz, *A.I.Ch.E.J.*, 1965, **11**, 121-130.